Dipole analyses of cosmic radio background with SKA

Tiziana Trombetti & Carlo Burigana

INAF-Istituto di Radioastronomia

CMB dipole

COBE

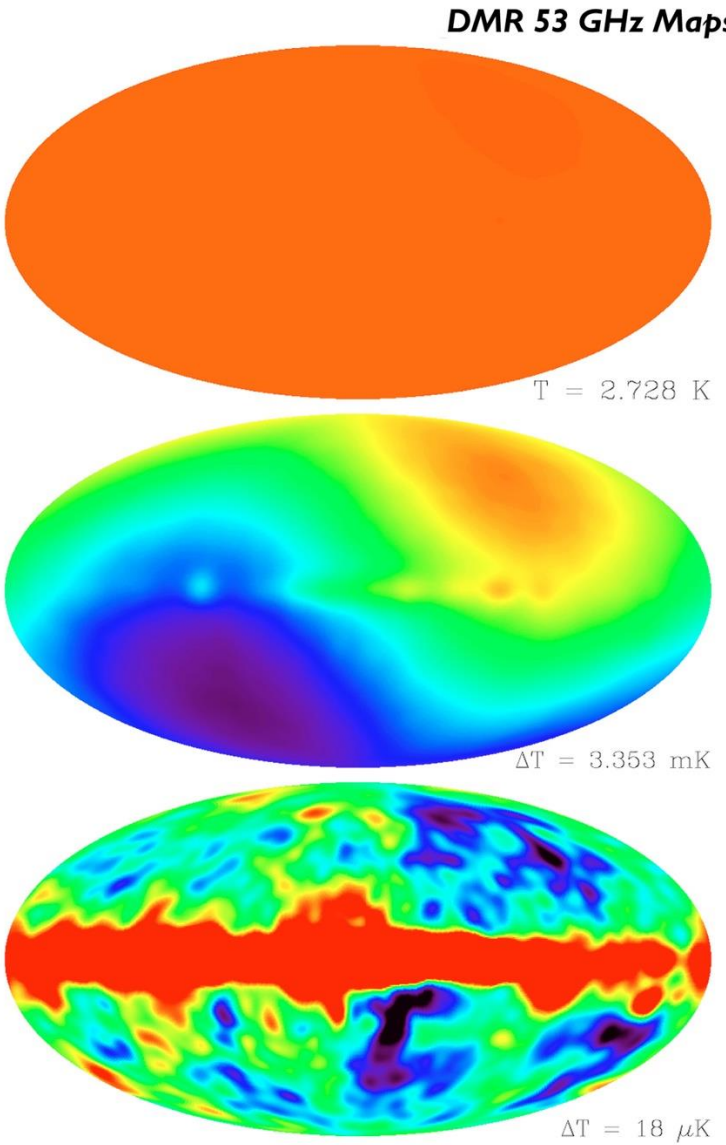

https://lambda.gsfc.nasa.gov/product/cobe/more_images/cobeslide29.jpg

WMAP

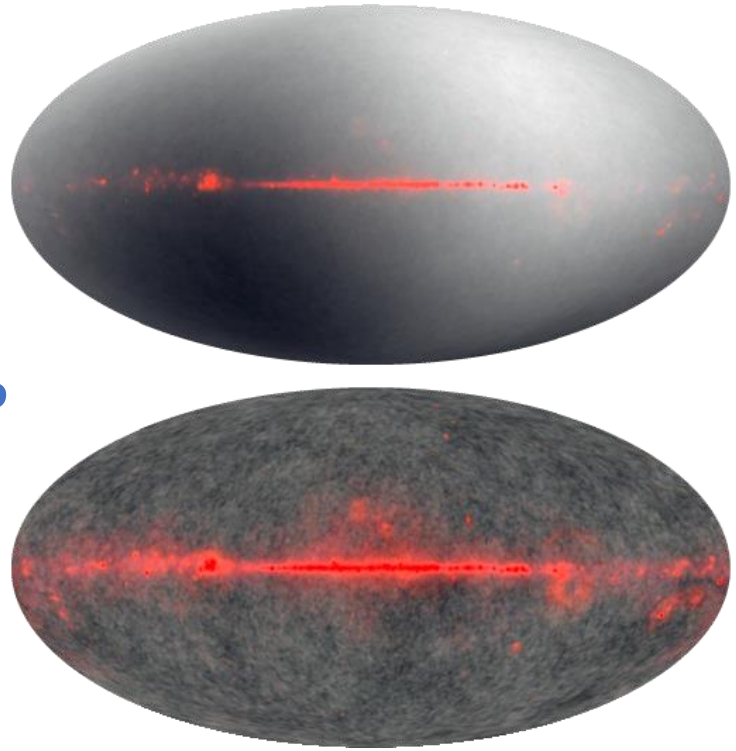

False color images. Q-band red, V-band green, W-band blue. A CMB therm spectrum grey.

Top: 3 color combination image from the Q-, V-, and W-band maps. Dipole and high Galactic latitude anisotropy are seen.

Bottom: similar but without dipole.

https://lambda.gsfc.nasa.gov/product/wmap/pub_papers/firstyear/basic/wmap_cb1_images.html

CMB dipole: *Planck … & beyond*

Dipole direction in Galactic coordinates
l=264.021°, b=48.253° v = (369.82 ± 0.11) km/s
$\beta = v/c \simeq 1.2336 \times 10^{-3} \simeq A_{dip} / T_0$
velocity of the Solar System barycentre with respect to the CMB
Planck Collaboration 2020, AA 641 A1

First confirmation of v with aberration & modulation (Challinor & van Leeuwen 2002, Sollom 2010) of CMB anisotropies
v= 384 km/s ± 78 km/s (stat.) ± 115 km/s (syst.)

Planck Coll. 2014, A&A 571, A27, Planck 2013 results. XXVII. Doppler boosting of the CMB: **Eppur si muove**

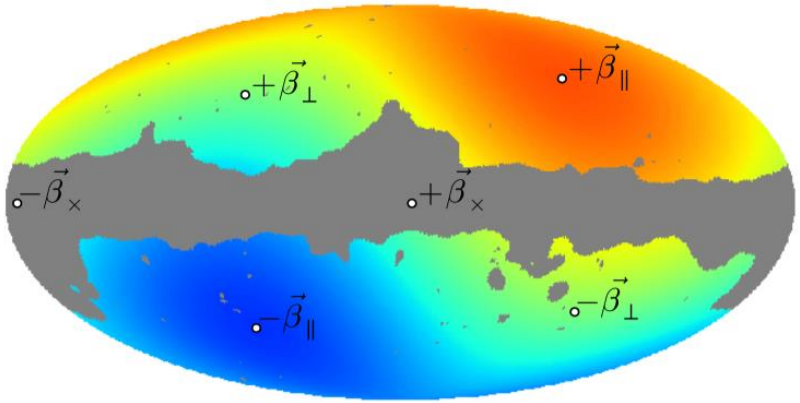

Fig. 2. Specific choice for the decomposition of the dipole vector $\boldsymbol{\beta}$ in Galactic coordinates. The CMB dipole direction $(l, b) = (263.^\circ99, 48.^\circ26)$ is given as $\boldsymbol{\beta}_\parallel$, while two directions orthogonal to it (and each other) are denoted as $\boldsymbol{\beta}_\perp$ and $\boldsymbol{\beta}_\times$. The vector $\boldsymbol{\beta}_\times$ lies within the Galactic plane.

- ❑ **We observe the CMB dipole, and we now firmly know from *Planck* that a significant part of it is kinetic**

But … is it almost fully kinetic or there is also a non negligible intrinsic dipole?

For many standard models the anisotropy power of intrinsic dipole and quadrupole is expected to be similar … but ...

- ✓ **CMB space missions observed a relatively low quadrupole (and also other types of low multipole anomalies)**
- ✓ **But, in principle, anisotropy power of intrinsic dipole may be larger**

- ❖ **CMB space missions like CORE could study boosting effects to polarization and cross-correlations → more robust determination of purely velocity-driven effects that are not degenerate with the intrinsic CMB dipole: overall S/N ≃ 13 (Burigana+ 2018)**

→ **Essentially as an ideal cosmic-variance-limited experiment up to $\ell \simeq 2000$**

- ❖ **Method based on the exploitation the leakage of the intrinsic dipole into the CMB monopole and quadrupole (Yasini & Pierpaoli 2017), e.g. with CMB space missions like PIXIE (Kogut+ 2016), FOSSIL (M8, Aghanim+ 2025) that recently passed ESA Phase 1 selection**

CMB vs matter dipole

Many galaxy surveys indicates that matter dipole ≠ CMB dipole

See e.g. N.J. Secrest + 2022, ApJL 937, L31 ***A Challenge to the Standard Cosmological Model***

NRAO VLA Sky Survey (NVSS; Condon et al. 1998)

Wide-field Infrared Survey Explorer (WISE; Wright et al. 2010)

See also Böhme+ , PRL, 135, 201001 (2025) for a recent analysis: source count dipole excess by a factor of 3.67±0.49 —> a 5.4σ discrepancy.

- ✓ **The large dipoles seen in radio galaxies & quasars independently reject, at 2.6σ & 4.4σ, the null hypothesis that the dipoles arise from Doppler boosting and relativistic aberration with velocity 370 km/s in the CMB dipole direction**
- ✓ **Dipole amplitudes are about 3 and 2 times larger than the respective kinematic expectations and point 45° and 26° from CMB dipole (l=264.021°, b=48.253°)**
- ✓ **The joint significance of this rejection of the cosmological principle is 5.1σ**
- ✓ **These anomalously large dipoles are statistically consistent with a single, shared dipole of distant galaxies and quasars, with amplitude $\mathcal{D}=(1.40\pm0.13)\times10^{-2}$ in the direction (l, b)=(233°±6°, 34°±5°)**
- ✓ **No evidence for a frequency dependence of the amplitude**
- ✓ **Agreement between radio galaxy & quasar dipoles improves by subtracting standard kinematic expectation: $\mathcal{D}=(0.86\pm0.14)\times10^{-2}$; (l, b)=(217°±10°, 20°±7°)**
- ✓ **Intrinsic overdensity of galaxies and quasars on very large scales, in a direction 48° away from the CMB dipole**

Observer motion → modification and transfer of the CB spectrum

$$T_{\rm th}^{\rm BB/dist}(\nu,\hat{n},\boldsymbol{\beta}) = \frac{xT_0}{\ln(1+1/(\eta(\nu,\hat{n},\boldsymbol{\beta}))^{\rm BB/dist})} \qquad (1)$$

observed signal map

$$\text{where } \eta(\nu,\hat{n},\boldsymbol{\beta}) = \eta(\nu') \text{ with } \nu' = \nu(1-\hat{n}\cdot\boldsymbol{\beta})/(1-\beta^2)^{1/2} \qquad (2)$$

Lorentz invariance of photon distribution function $\eta(\nu)$

$\hat{n}$ sky direction unit vector associated to polar coordinates (colatitude) and (longitude)

$\boldsymbol{\beta} = \mathrm{v}/\mathrm{c}$

N.B.: monopole background is by definition the isotropic component – no aberration

Compton-Getting effect (Forman, M. A. 1970, Planet. Space Sci., 18, 25)

$$T_{\rm th}^{\rm BB/dist}(\nu,\theta,\phi,\beta) = \sum_{\ell=0}^{\ell_{\rm max}} \sum_{m=-\ell}^{\ell} a_{\ell,m}(\nu,\beta) Y_{\ell,m}(\theta,\phi) \qquad (3)$$

$Y_{\ell,m}(\theta,\phi)$ spherical harmonics, related to associated Legendre Polynomial $P_\ell^m(\cos\theta)$

$$Y_{\ell,m}(\theta,\phi) = \tilde{P}_\ell^m(\cos\theta) \qquad \tilde{P}_\ell^m(\cos\theta) = \sqrt{\frac{2\ell+1}{4\pi}\frac{(\ell-m)!}{(\ell+m)!}} P_\ell^m(\cos\theta) \qquad (4)$$

renormalized associated Legendre Polynomial

when $m=0$

- ✓ We adopt a reference system with the z axis parallel to the observer velocity
- ✓ Adopting a reference system with the z axis parallel (or antiparallel) to the observer velocity, we are interested only in the non-vanishing coefficients with $m = 0$
- ✓ The publicly available tools (e.g. HEALPix, Górski et al. 2005) allow us to efficiently compute the $a_{\ell,m}$ coefficients passing from a reference system to another
- ✓ See Goldstein, J. D. 1984, J. Geophys. Res., 89, 4413 for transformations of spherical harmonics coefficients under rotation

Azimuthal symmetry simplification

Solution in terms of derivatives

T. Trombetti+ 2024

Let us assume that $T_{th}^{BB/dist}(w)$ with $w = \cos\theta$ can be expanded in Taylor's series around $w = \cos(\pi/2)=0$

i.e. the direction perpendicular to observer motion;

$T^{(0)}_{th}$, $T^{'}_{th}$, ..., $T^{(6)}_{th}$ derivatives with respect to w evaluated at $w = 0$

$$a_{0,0} = \sqrt{4\pi}\left[T_{th}^{(0)} + \frac{1}{6}T_{th}'' + \frac{1}{120}T_{th}^{(4)} + \frac{1}{5040}T_{th}^{(6)}\right]$$

monopole: observed ≠ intrinsic

$$a_{1,0} = \sqrt{\frac{4\pi}{3}}\left[T_{th}' + \frac{1}{10}T_{th}''' + \frac{1}{280}T_{th}^{(5)}\right],$$

$$a_{2,0} = \frac{1}{3}\sqrt{\frac{4\pi}{5}}\left[T_{th}'' + \frac{1}{14}T_{th}^{(4)} + \frac{1}{504}T_{th}^{(6)}\right],$$

$$a_{3,0} = \frac{1}{15}\sqrt{\frac{4\pi}{7}}\left[T_{th}''' + \frac{1}{18}T_{th}^{(5)}\right],$$

$$a_{4,0} = \frac{1}{105}\sqrt{\frac{4\pi}{9}}\left[T_{th}^{(4)} + \frac{1}{22}T_{th}^{(6)}\right],$$

$$a_{5,0} = \frac{1}{945}\sqrt{\frac{4\pi}{11}}\,T_{th}^{(5)},$$

$$a_{6,0} = \frac{1}{10395}\sqrt{\frac{4\pi}{13}}\,T_{th}^{(6)},$$

Separation: odd / even ℓ & derivatives

≈ Danese & De Zotti 1981 but there using $\theta=0$ and $\theta=\pi/2$

$$D_\ell = (2\ell - 1)D_{\ell-1}, \text{ with } D_0 = 1$$

denominator in front of square root

Signal given with respect to v

Link between derivatives respect to w with derivatives with respect to v

$$\nu' = \nu(1 - \beta w)/(1 - \beta^2)^{1/2}$$

$$\frac{dT_{th}}{dw} = \frac{dT_{th}}{d\nu'}\frac{d\nu'}{dw} = \frac{dT_{th}}{d\nu'}\frac{-\beta\nu}{(1-\beta^2)^{1/2}}$$

$-\beta\nu/(1-\beta^2)^{1/2}$ does not contain w,

$$\frac{dT_{th}^n}{dw^n} = \frac{dT_{th}^n}{d\nu'^n}\left[\frac{-\beta\nu}{(1-\beta^2)^{1/2}}\right]^n$$

Approximate scaling as β^n

Changing β

For a speed $\beta_a \neq \beta$ (ex. $\beta_a > \beta$), defining $f_a = \beta_a/\beta$ (ex. $f_a > 1$), the ratio between the derivatives computed for these two speeds is:

$$\frac{T_{th}^{(n)}\big|_\beta}{T_{th}^{(n)}\big|_{\beta_a}} = f_a^{-n}\left(\frac{1-\beta_a^2}{1-\beta^2}\right)^{n/2} R_n$$

$$R_n = \left(\frac{dT_{th}^n}{d\nu'^n}\Big|_{\nu'_{\beta,\perp}}\right)\left(\frac{dT_{th}^n}{d\nu'^n}\Big|_{\nu'_{\beta a,\perp}}\right)^{-1} \simeq 1$$

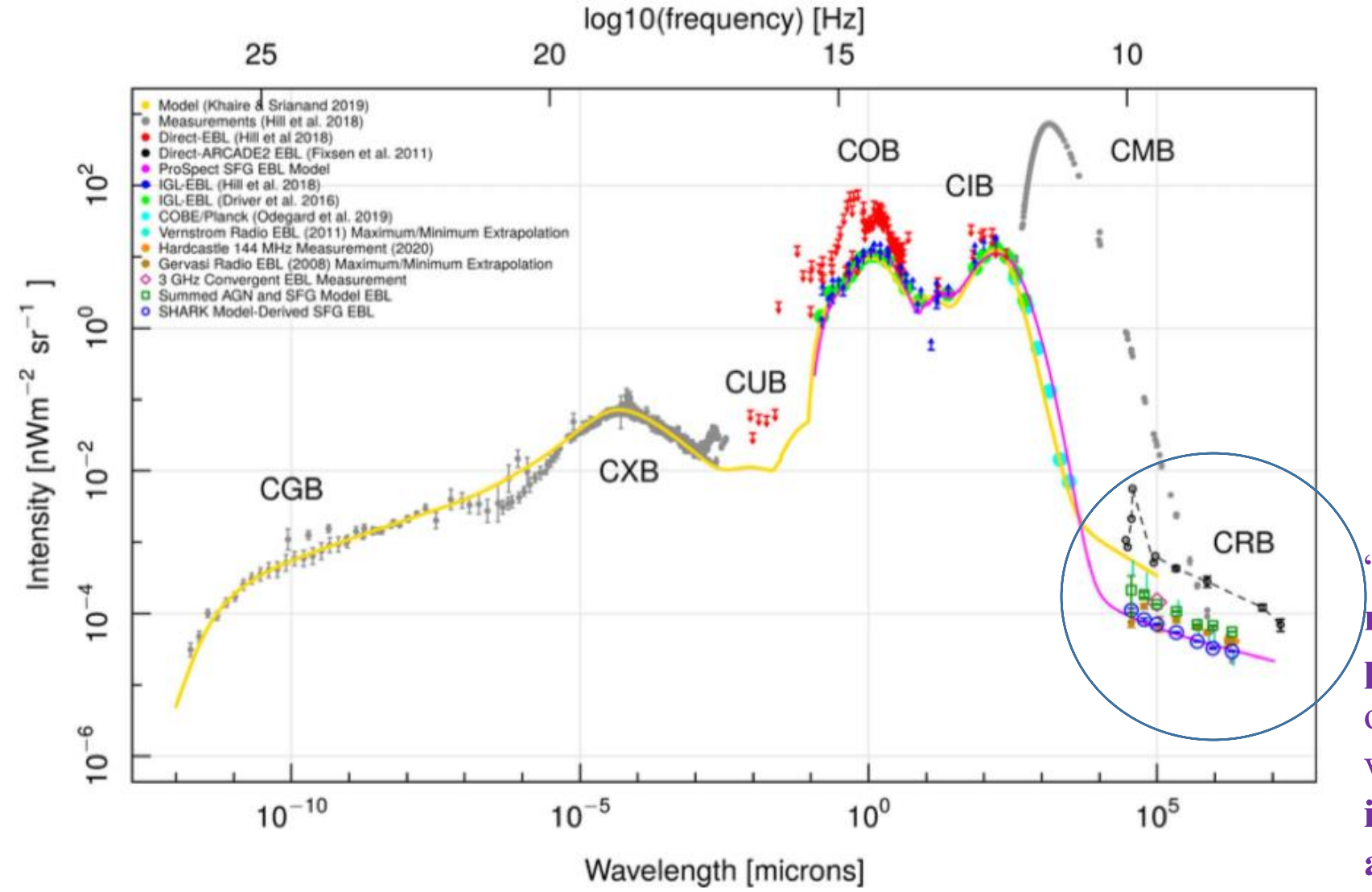

Figure 7. The complete EBL over the entire measured EM range, including our discrete radio source count measurements along with those from the literature (as indicated in the legend). Also shown is the CMB contribution which dominates at most radio wavelengths and the constraints on the total non-CMB radio EBL from ARCADE2 (black dotted line and open circles). Our model-derived (extrapolated) data points in the radio region are shown as green squares (AGN and SFG) and blue circles (SFG). The solid purple line is the best fitting (dotted) SFG only prediction from Fig. 6.

Cosmic Background Spectrum

Tompkins, S. A., et al. 2023, MNRAS, 521, 332

The cosmic radio background from 150 MHz to 8.4 GHz and its division into AGN and star-forming galaxy flux

"We can **rule out a significant missing discrete source radio population** and suggest that the cause of the high ARCADE-2 radio-EBL values may need to be sought **either in the foreground subtraction or as a yet unknown diffuse component in the radio sky**."

Monopole & Dipole Spectrum

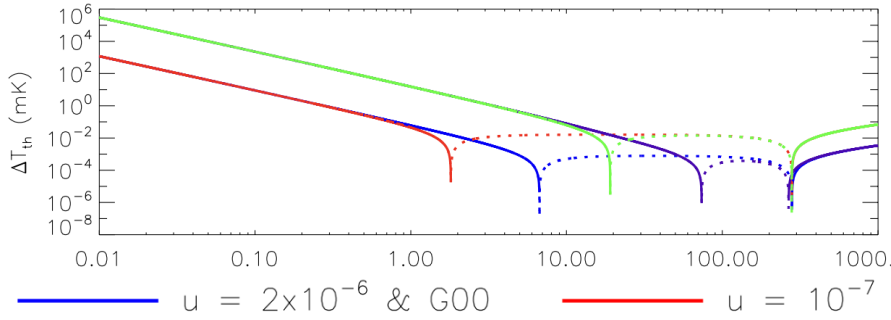

Late

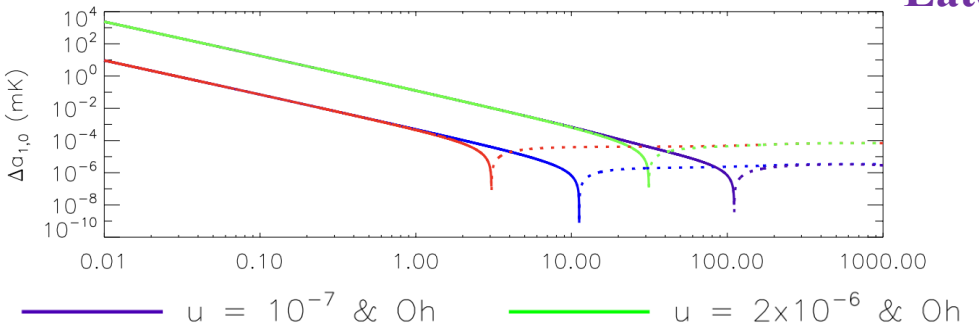

Extragalactic Sources Radio Background

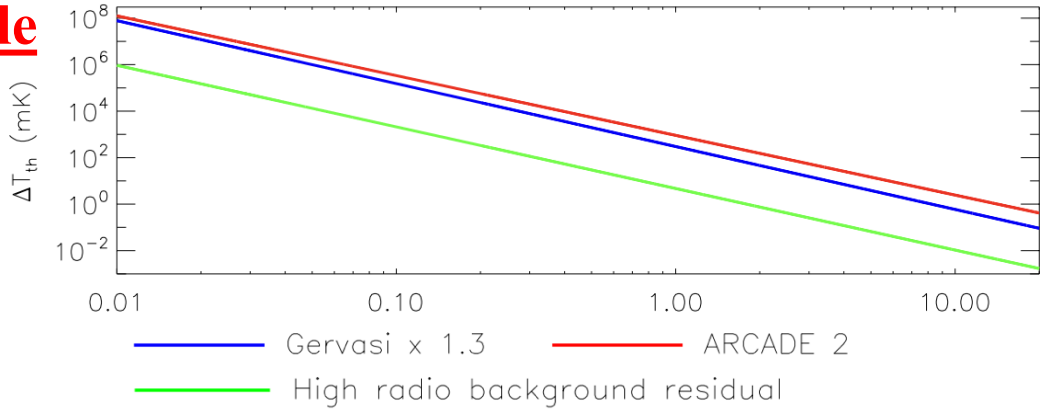

Dominant Background In the Radio

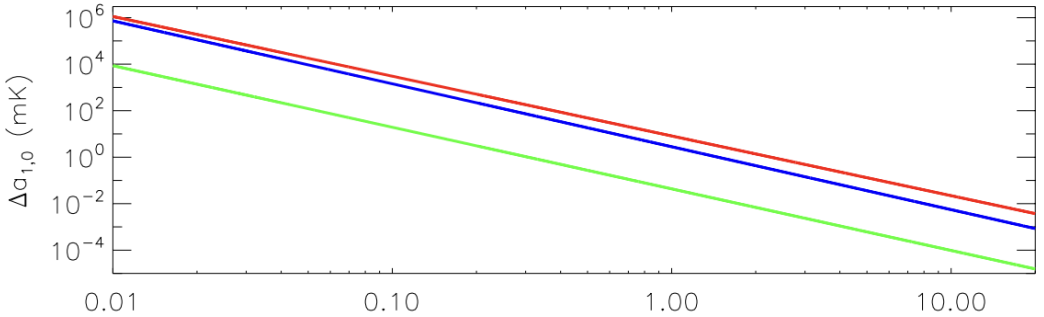

CMB Distortions

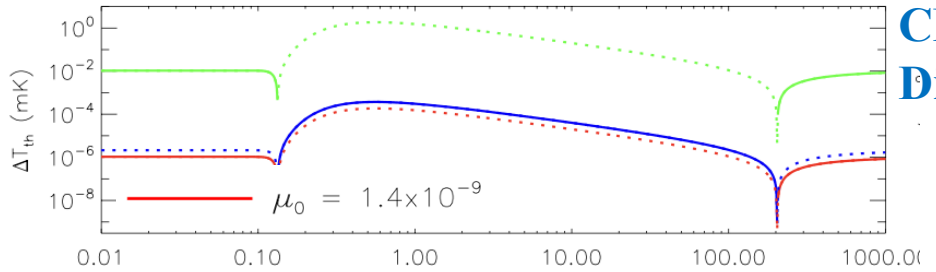

Redshifted 21 cm line

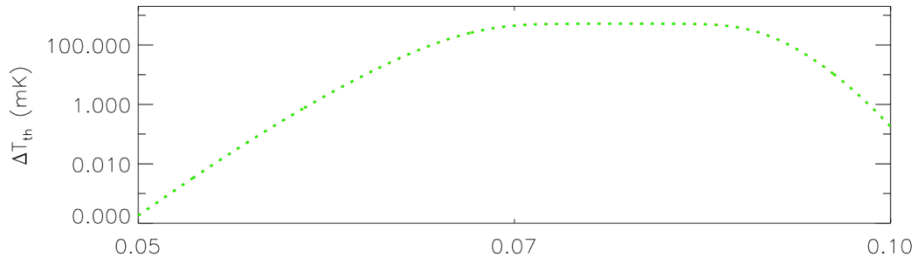

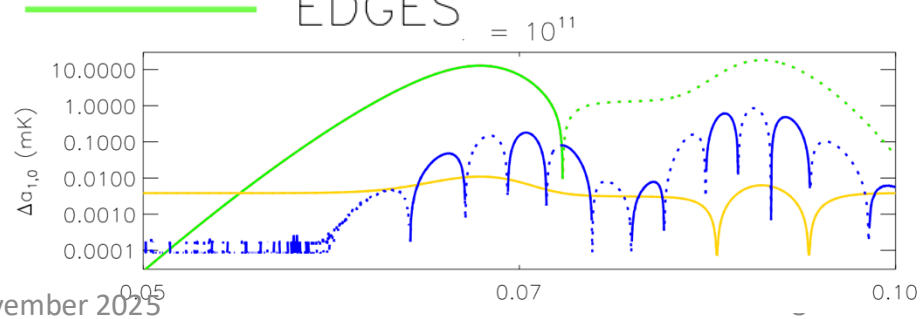

Early

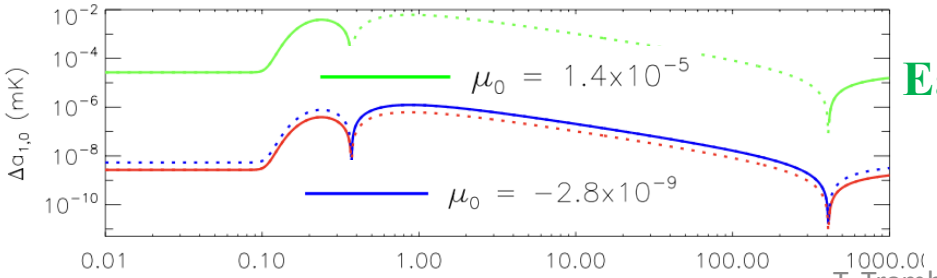

From Trombetti+ 2021, AA 646, A75

Dipole sensitivity on patches

Sensitivity on 2 arcmin pixel, 1 day of integration, 10 or 40 MHz band

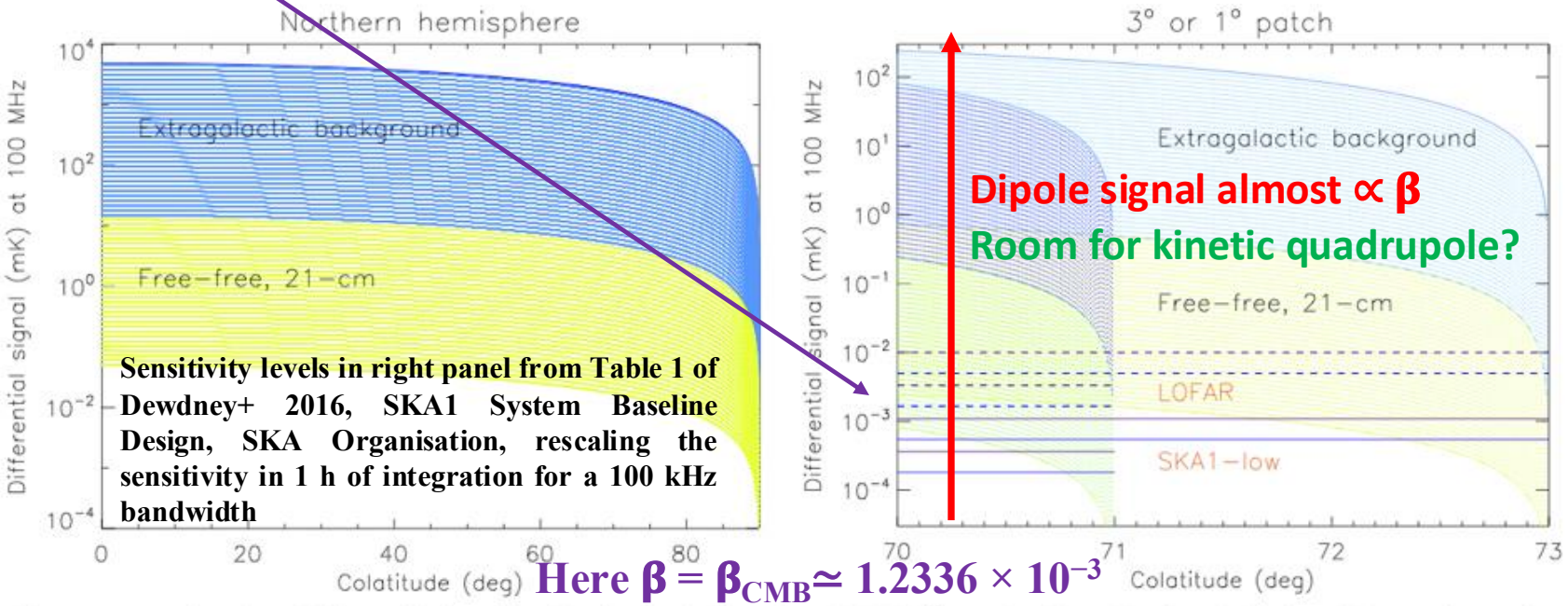

Sensitivity levels in right panel from Table 1 of Dewdney+ 2016, SKA1 System Baseline Design, SKA Organisation, rescaling the sensitivity in 1 h of integration for a 100 kHz bandwidth

Here $\beta = \beta_{CMB} \simeq 1.2336 \times 10^{-3}$

Fig. 5: Range of predicted differential signal for the dipole, $\Delta T(\theta) = \Delta a_{\ell,0} [3/(4\pi)]^{1/2} \cos\theta$, where θ is the colatitude and $\Delta a_{\ell,0}$ refers to the dipole harmonic component ℓ=1, m=0 in a frame with the z-axis parallel to the observer motion, after the subtraction of the standard CMB blackbody, in order to emphasize the interesting signal (here at 100 MHz and in equivalent thermodynamic temperature). The higher part of the blue areas refers to estimates of the signals for the diffuse background from extragalactic radiosources [see e.g. Trombetti+ 2021]; in the lower part it is assumed that sources above certain detection thresholds are subtracted. Yellow areas refer to estimates of the signals for the diffuse free-free distortion, from the minimal prediction accounting for the diffuse IGM contribution to the maximum level corresponding to the integrated contribution from ionized halos, and for various models of the IGM 21-cm redshifted HI line [e.g. Cohen+ 2017]. *Left panel*: the case of an all-sky survey, displayed for simplicity only for a hemisphere. *Right panel*: a zoom of left panel for a patch of 3° (1°); here we display $\Delta T(\theta) - \Delta T(\theta_*)$, with θ_* = 73° (71°), i.e. the differential signal inside the patch, to be compared with typical sensitivity levels (see also text in Milestones) for LOFAR (dashed lines) and SKA1-low (solid lines) in a nominal pixel of 2 arcmin for one day of integration in the patch. Violet (blue) lines assumes a bandwidth of 10 (40) MHz to appreciate spectral shapes of the 21-cm redshifted HI line (the other types of signal).

Simple estimate: **along a meridian in a reference frame with z-axis parallel to the dipole direction, the signal variation at colatitude θ from a dipole pattern with amplitude ΔT in a limited sky area of linear size Δθ, has an amplitude $|\Delta T_{\Delta\theta}| \simeq \Delta T \cdot (\Delta\theta/90°) \sin\theta$, with $\sin\theta \simeq 1$ at angles large enough from the poles**

patch

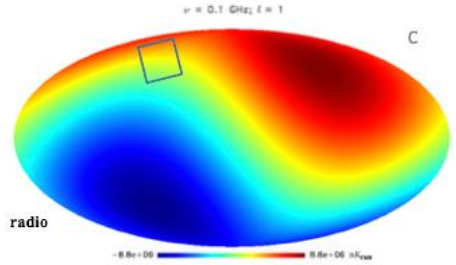

- ✓ **Dealing with almost independently observed sky patches (e.g. interferometric techniques)**
- ✓ **In principle, for extreme sensitivities, dipole pattern reconstruction could be carried out not necessarily requiring a coherent sky mapping up to the largest scales [Trombetti & Burigana 2019]**
- ✓ **For example, considering ~50-100 MHz sensitivities to the diffuse signal with forthcoming and future projects**
  - **~ several tens of mK could allow to identify the extragalactic background**
  - **from ~ a few μK to ~ mK it could be possible to study the reionization imprints**

Frequency Range SKA-mid (GHz): 0.35 - 14

Sensitivity @ 100 kHz band

Rescaled to 4 GHz bandwidth @ 10GHz

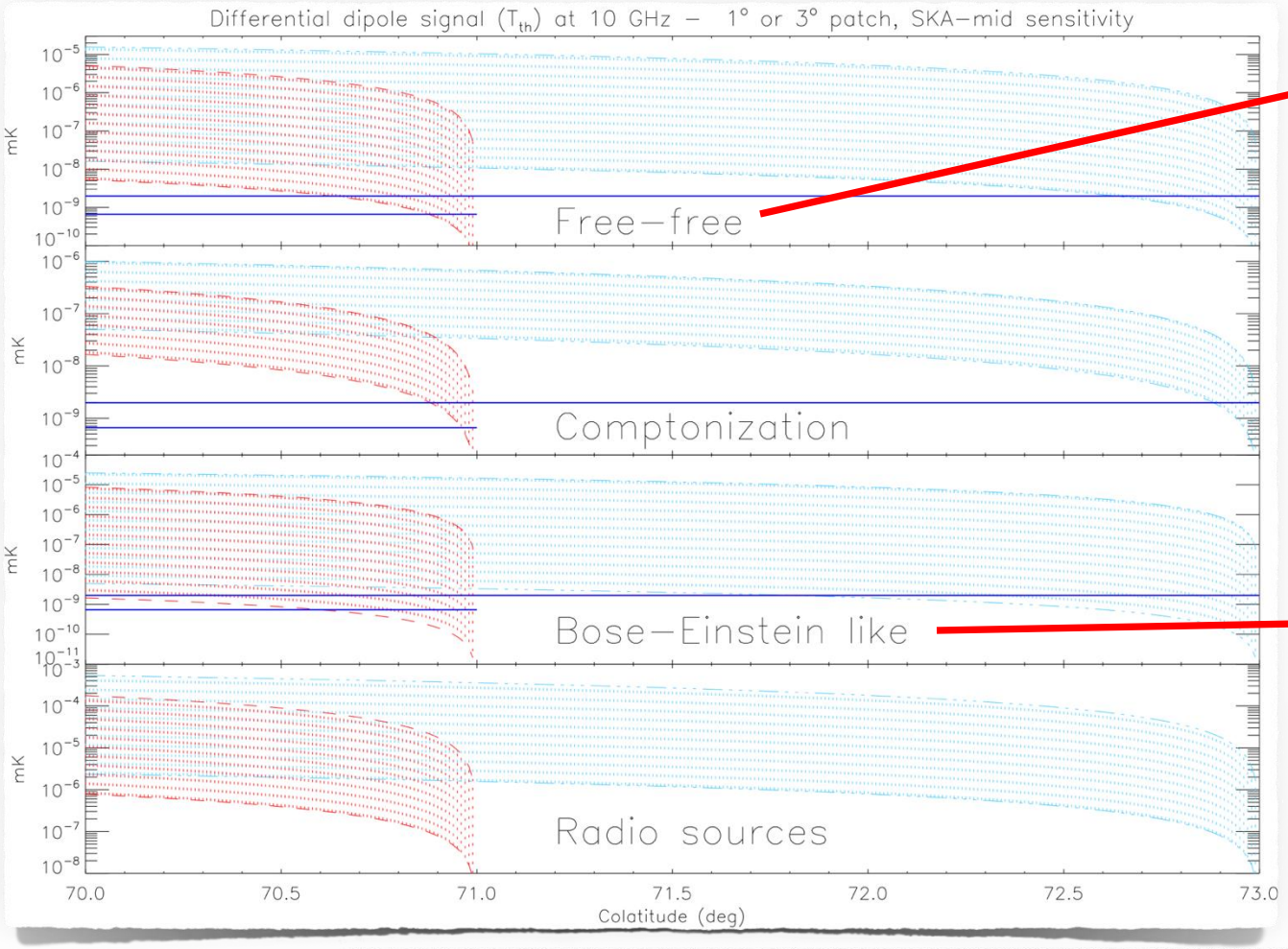

Free-free

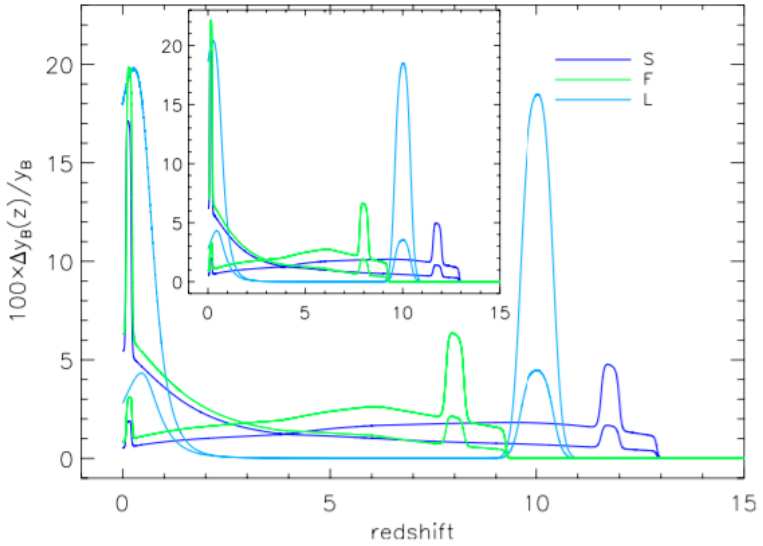

Figure 14. Redshift dependence of the partial contribution to the free–free parameter, evaluated per redshift bin $\Delta z = 0.2$ at each z for $k_{max} = 100$ (and $k_{max} = 500$ in the inset). Being normalized to the global value of y_B at each wavelength, $\Delta y_B(z)/y_B$ turns to be essentially independent of the wavelength, thus we present only the result at 10 cm. The dashed–dotted lines display the results found neglecting the clumping, for the corresponding histories reported in legend.

Trombetti & Burigana 2014

BE: $z \sim 10^3$ recombination or
$z > 10^5$ kinetic equilbrium era

Observations & needs

- ✓ ensamble of independent patches, or
- ✓ sky areas from patch assembling with mosaicing techniques to increase differential signal
- ✓ multifrequency (SKA low & mid)

- keeping information on largest scales in the patch or patch assembling (short baselines)

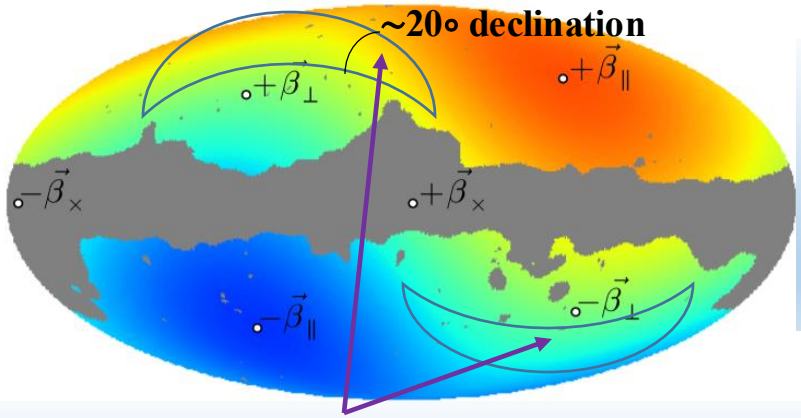

GOOD SKY REGIONS?

Favourite regions accessible to SKA for patch selection should be far enough from:

- ✓ Galactic plane, to avoid large contamination
- ✓ maximum & minimum of dipole, because $|\Delta T_{\Delta\theta}| \simeq \Delta T \cdot (\Delta\theta/90°)\ \sin\theta$
- ✓ bright sources, to avoid large contamination

- Above sensitivities are based on 1.6 (0.18) min of integration on 2 arcmin pixel of a 1deg (3 deg) side patch

- ✓ Likely instrument noise dominated
- ✓ … but depending on sky area/direction check for source confusion noise

❑ Galactic signal subtraction

➢ Galactic modeling

➢ Component separation of diffuse signals using multifrequency data
(various methods, blind and parametric, have been elaborated …)

➢ Considering more patches to increase statistics and mitigate susceptibility to foreground Galactic modeling
(… cosmological signal should come from the same dipole pattern in all patches)

➢ Simulations

CMB: nearly all-sky, moderate resolution
SKA: limited sky areas, very high resolution

Potential impact of Galactic diffuse foregrounds

Simulated sky in pixel (p) space

- **Theoretical model (T) including boosting with monopole & dipole (& subdominant terms, quadrupole, …)**
  We consider the **Extragalactic Sources Radio Background** (adopting here the Gervasi+ 2008 model x 1.3)

+

- Instrumental Noise (IN) + Source Confusion Noise (SCN)
  - random Gaussian (RG), with zero mean & variance per pixel *from SKA specifications/sensitivity calculator*

+

- Potential Residuals from Galactic diffuse foregrund (G), (parametrically, E_{for} & $E_{for,syst}$) modelled with two terms:
  - ✓ Stochastic, proportional to Galactic signal amplitude
  - ✓ Systematic, fully correlated with / proportional to Galactic signal

Not so critical

Critical term

→ $S(p) = T(p) + (IN(p) + SCN(p)) + E_{for} \cdot RG(p) \cdot |G(p)| + E_{for,syst} \cdot G(p)$

Linear fitting on patches

- Masking according to SKA Low and SKA Mid (band 2) typical Phase 1 cosmological surveys
  (D.J. Bacon +, Cosmology with Phase 1 of the Square Kilometre Array: Red Book 2018: Technical specifications and performance forecasts, PASA)

- Fitting just monopole & dipole: linear fit in cos(colatitude) with z // motion →
  intercept → Monopole ; slope → Dipole ; their ratio → v *(@ first order)*

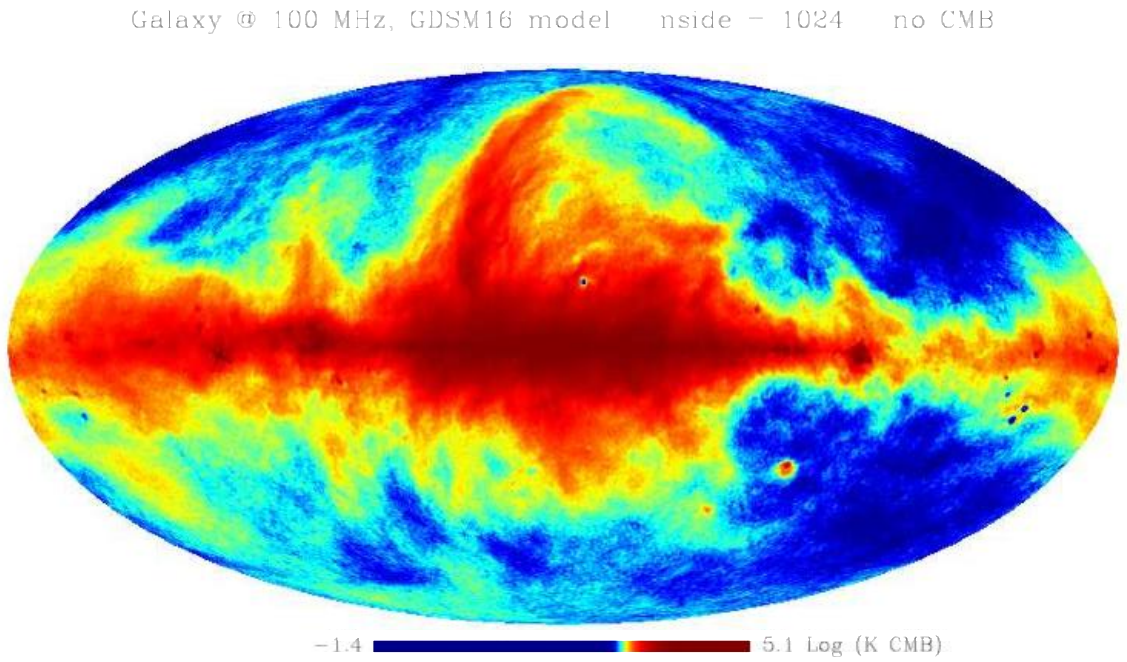

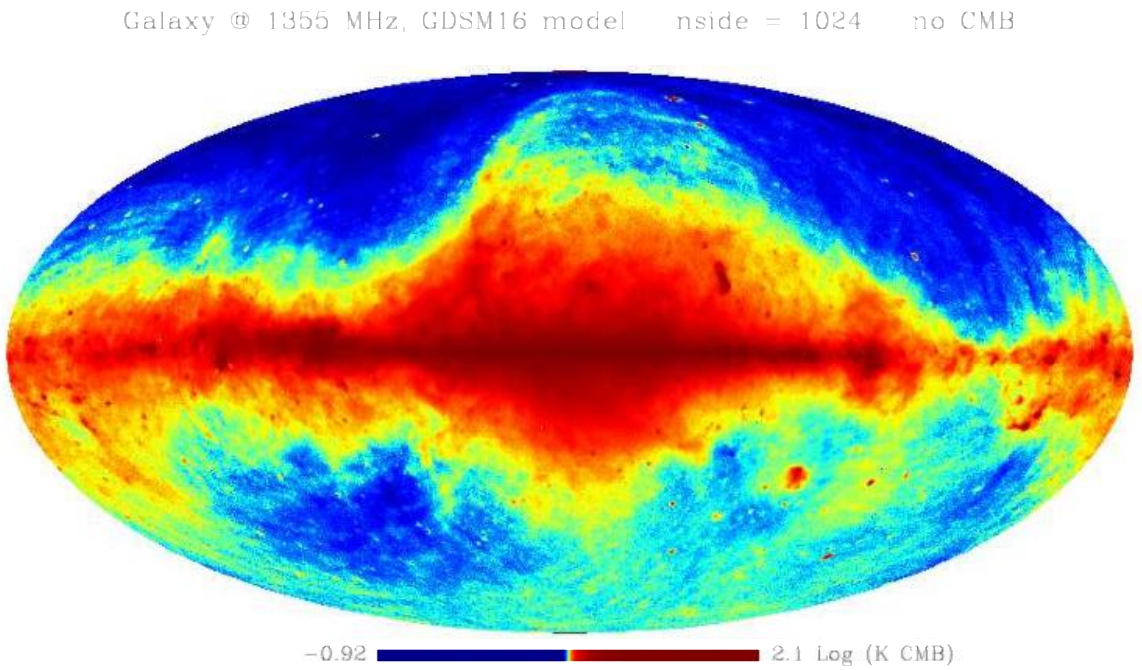

Diffuse Galactic emission model

@ SKA Low @ 100 MHz and SKA Mid band 2 @ 1.355 GHz from

"An improved model of diffuse galactic radio emission from 10 MHz to 5 THz", H. Zheng +, 2016, MNRAS

maps @ n_{side}=1024, HEALPix, Gorski+ 2005, 3.4 arcmin

Simulation @ 100 MHz

Test with sensitivity corresponding an integration per FoV of 24h << t_{int} planned for Deep SKA1-LOW Survey

AA*

AA*
307

Degrees
Right Ascension * 51.6 deg
Declination * -56.0 deg
Minimum Elevation * 20

Continuum

Integration Time * 2.8658951e-5 hours
Central Frequency * 100 MHz
Continuum Bandwidth * 40 MHz
Number of sub-bands * 4
Spectral Resolution 5.43 kHz (16.3 km/s)
Spectral Averaging * 1
Effective resolution 5.43 kHz (16.3 km/s)
Image Weighting * Briggs
Robust Value 0

Results

Weighted continuum sensitivity
4.75 mJy/beam (1.31)†
Continuum confusion noise
62.49 uJy/beam
Total continuum sensitivity
4.75 mJy/beam
Continuum synthesized beam-size
18.1" x 14.8"
Continuum surface-brightness sensitivity
2160.16 K

Weighted sensitivity per sub-band
10.78 mJy/beam - 8.98 mJy/beam (1.31)†
Confusion noise per sub-band
95.20 uJy/beam - 43.23 uJy/beam
Total sensitivity per sub-band
10.78 mJy/beam - 8.98 mJy/beam
Synthesized beam-size per sub-band
21.3" x 17.4" - 15.7" x 12.9"
Surface-brightness sensitivity per sub-band
4906.14 K - 4085.64 K

Weighted spectral sensitivity
394.40 mJy/beam (1.36)‡
Spectral confusion noise
62.54 uJy/beam
Total spectral sensitivity
394.40 mJy/beam
Spectral synthesized beam-size
18.2" x 14.8"
Spectral surface-brightness sensitivity
179331.56 K

FWHM of the RMSF
0.4 rad/m²
Maximum Faraday depth extent
0.5 rad/m²
Maximum Faraday depth
909.4 rad/m²

† Weighting correction factor (30% bandwidth)
‡ Weighting correction factor (single channel)

AA* only 1.7 times less sensitive than AA4 → no problem!

AA4

Subarray Configuration * AA4
Number of Stations 512

Degrees
Right Ascension * 51.6 deg
Declination * -56.0 deg
Minimum Elevation * 20

Continuum

Integration Time * 2.8658951e-5 hours
Central Frequency * 100 MHz
Continuum Bandwidth * 40 MHz
Number of sub-bands * 4
Spectral Resolution 5.43 kHz (16.3 km/s)
Spectral Averaging * 1
Effective resolution 5.43 kHz (16.3 km/s)
Image Weighting * Briggs
Robust Value 0

Results

Weighted continuum sensitivity
2.80 mJy/beam (1.29)†
Continuum confusion noise
63.39 uJy/beam
Total continuum sensitivity
2.80 mJy/beam
Continuum synthesized beam-size
18.8" x 14.5"
Continuum surface-brightness sensitivity
1255.51 K

Weighted sensitivity per sub-band
6.36 mJy/beam - 5.29 mJy/beam (1.29)†
Confusion noise per sub-band
96.55 uJy/beam - 43.87 uJy/beam
Total sensitivity per sub-band
6.36 mJy/beam - 5.29 mJy/beam
Synthesized beam-size per sub-band
22.1" x 17.1" - 16.3" x 12.6"
Surface-brightness sensitivity per sub-band
2851.24 K - 2374.28 K

Weighted spectral sensitivity
230.91 mJy/beam (1.33)‡
Spectral confusion noise
67.78 uJy/beam
Total spectral sensitivity
230.91 mJy/beam
Spectral synthesized beam-size
19.5" x 15.0"
Spectral surface-brightness sensitivity
96668.37 K

FWHM of the RMSF
0.4 rad/m²
Maximum Faraday depth extent
0.5 rad/m²
Maximum Faraday depth
909.4 rad/m²

for the same resolution element

← →

AA4 core only

AA4 (core only)
224

Degrees
Right Ascension * 51.6 deg
Declination * -56.0 deg
Minimum Elevation * 20

Continuum

Integration Time * 2.8658951e-5 hours
Central Frequency * 100 MHz
Continuum Bandwidth * 40 MHz
Number of sub-bands * 4
Spectral Resolution 5.43 kHz (16.3 km/s)
Spectral Averaging * 1
Effective resolution 5.43 kHz (16.3 km/s)
Image Weighting * Briggs
Robust Value 0

Results

Weighted continuum sensitivity
8.28 mJy/beam (1.67)†
Continuum confusion noise
58.69 mJy/beam
Total continuum sensitivity
59.27 mJy/beam
Continuum synthesized beam-size
490.4" x 406.5"
Continuum surface-brightness sensitivity
36.34 K

Weighted sensitivity per sub-band
18.81 mJy/beam - 15.66 mJy/beam (1.67)†
Confusion noise per sub-band
95.04 mJy/beam - 38.24 mJy/beam
Total sensitivity per sub-band
96.88 mJy/beam - 41.32 mJy/beam
Synthesized beam-size per sub-band
576.9" x 478.2" - 426.4" x 353.5"
Surface-brightness sensitivity per sub-band
59.40 K - 25.33 K

Weighted spectral sensitivity
614.04 mJy/beam (1.55)‡
Spectral confusion noise
63.67 mJy/beam
Total spectral sensitivity
617.33 mJy/beam
Spectral synthesized beam-size
508.3" x 420.2"
Spectral surface-brightness sensitivity
353.19 K

FWHM of the RMSF
0.4 rad/m²
Maximum Faraday depth extent
0.5 rad/m²
Maximum Faraday depth
909.4 rad/m²

Warning: You are approaching the confusion limit given the synthesized beam-size and frequency.

AA4 (core only) about 80 times less sensitive than AA4 … but confusion noise → about 600 times less sensitive than AA4

Simulation @ 1.355 GHz Mid band 2

Test with sensitivity corresponding an integration of 10000 h on 5000 sq. deg planned for Medium-Deep Band 2 Survey

Where? How?

N.B. integration time of Wide Band 1 Survey SKA1-Mid in Band 1 approximately 10000 hrs on 20000 sq. deg, i.e. about half sky

Bacon+2020

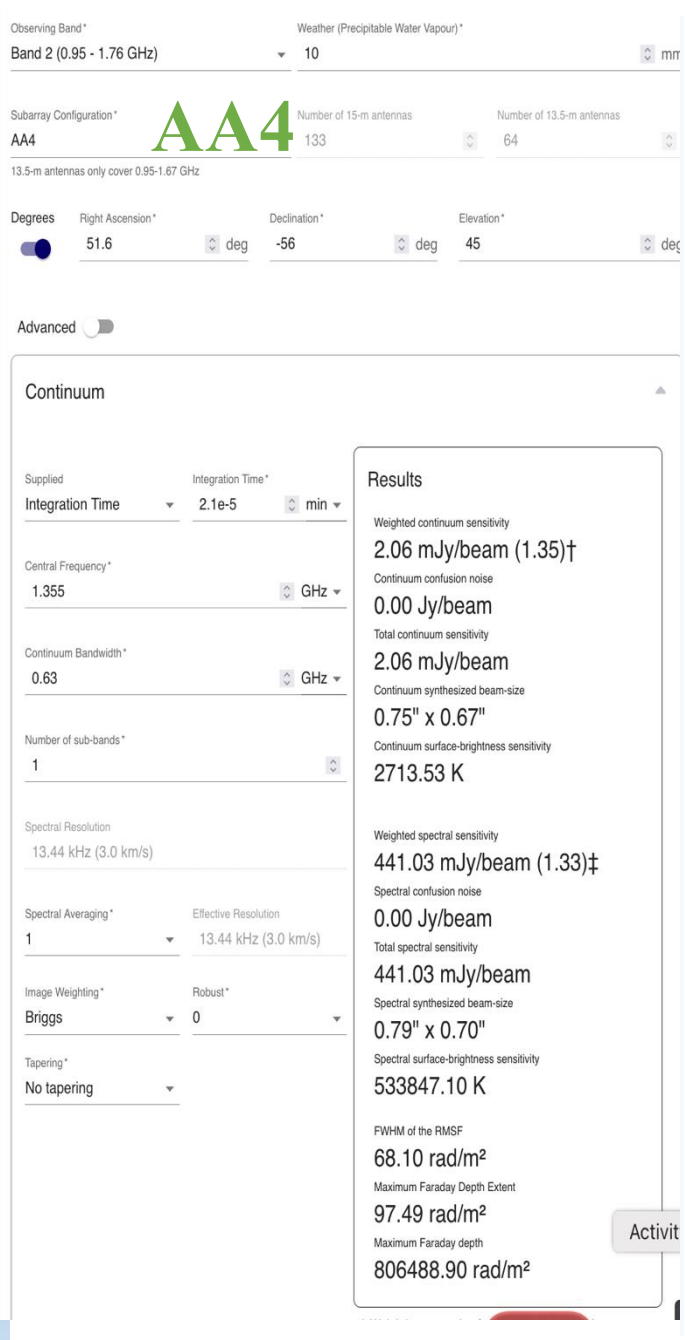

AA4

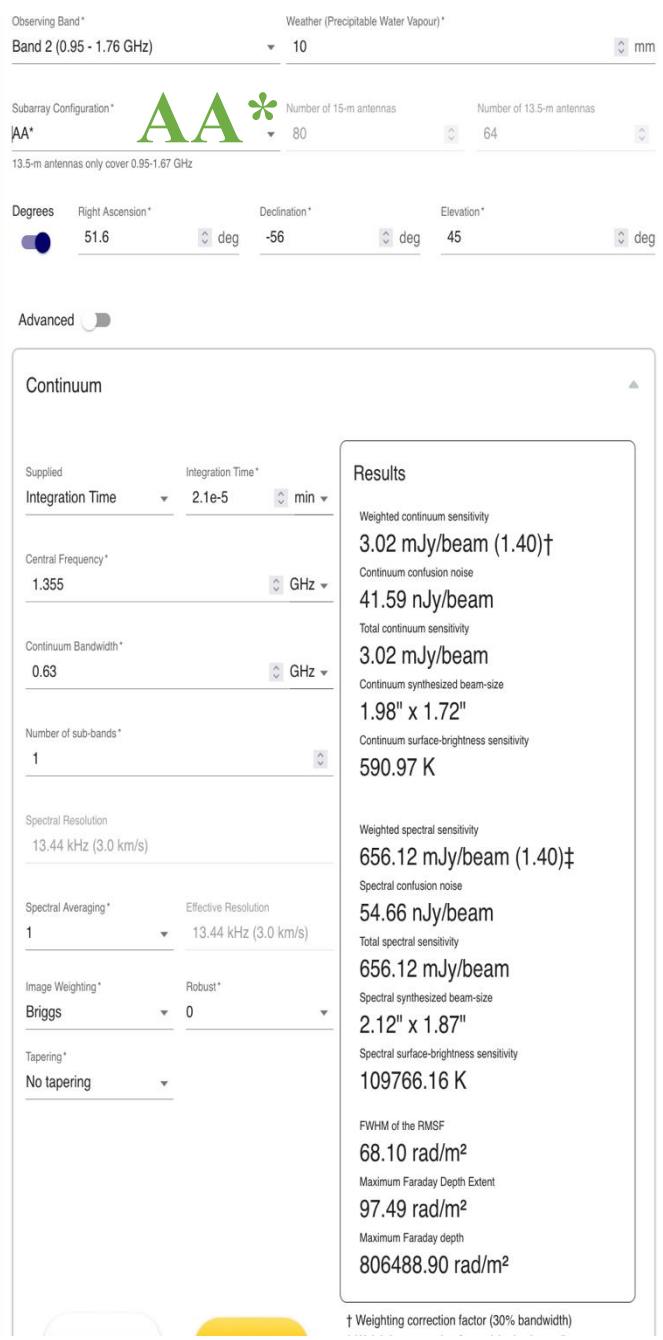

AA*

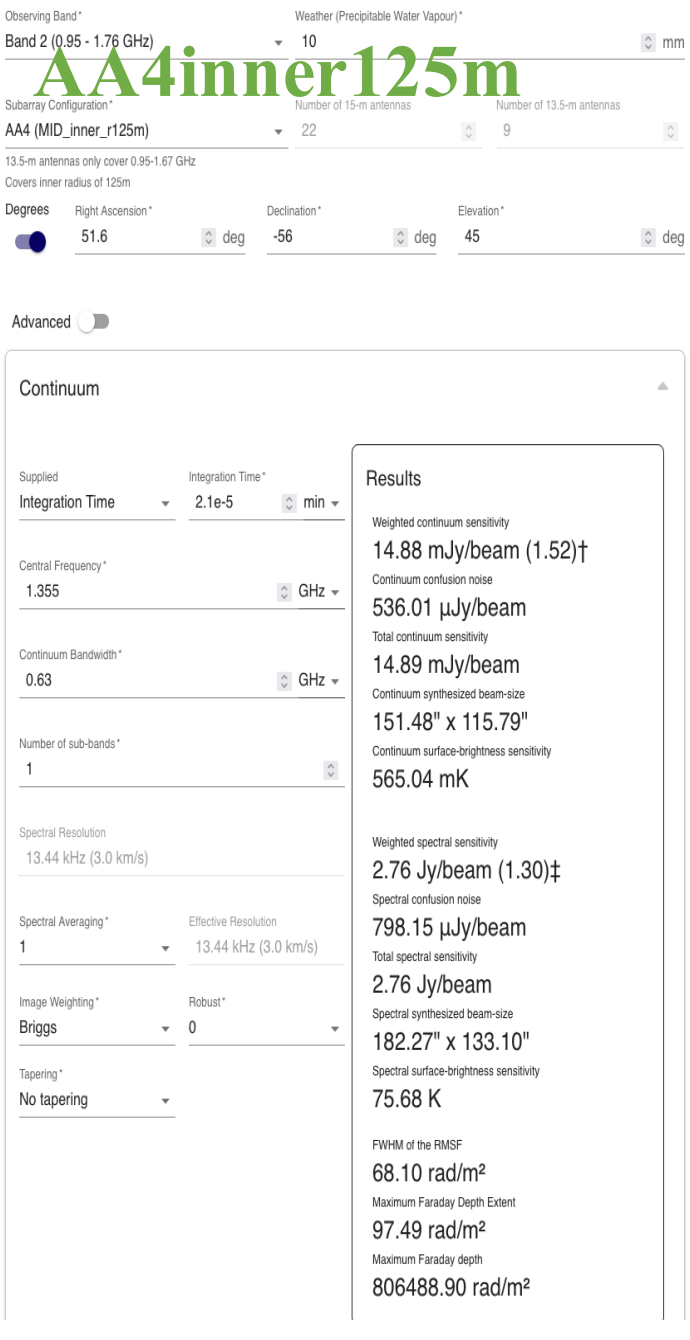

AA4inner125m

“Good” sky regions - Results @ 100 MHz & 1.355 GHz

Stochastic residuals only: $E_{for} = 0.05$

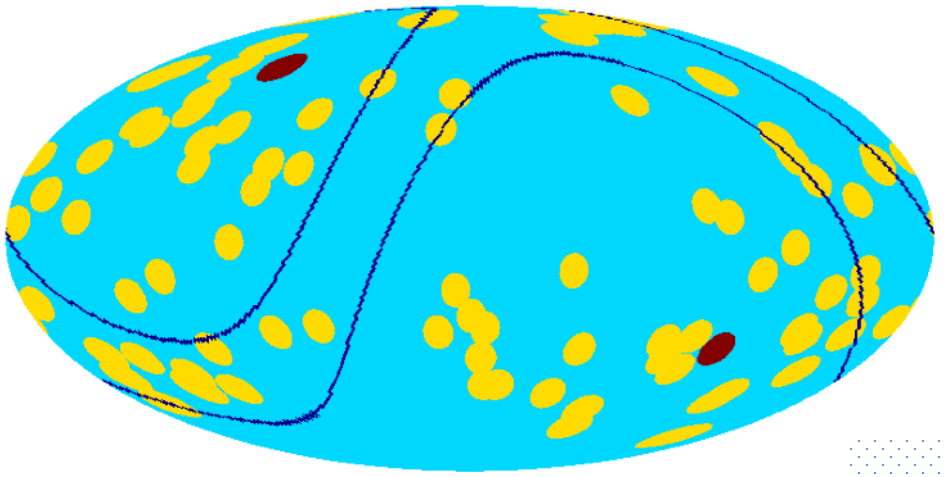

Blue lines corresponding to Dec of 30◦, 0◦
(Galactic coords, Mollweide projection)

100 MHz - Rel Err on v <= 5%
60 and 30 patches
respectively for the two cuts in declinations,
with a retrieved relative error on β, on average,
of about 2.3%

Considering 49152
(n_{side}=64, HEALPix, Gorski+ 2005)
centres of 100 sq deg circular patches

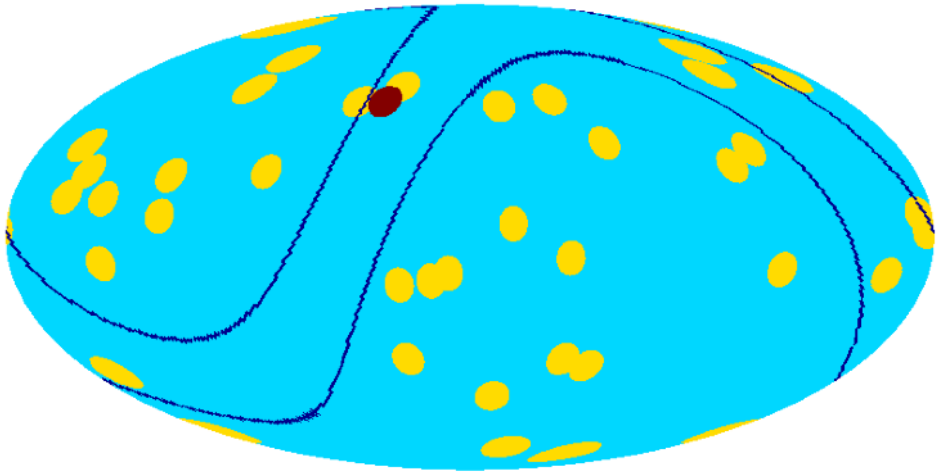

1.355 GHz - Rel Err on v <= 10%
26 and 18 patches
respectively for the two cuts in declinations,
with a retrieved relative error on β, on average,
of about 5.8%

“Good” sky regions - Results @ 100 MHz & 1.355 GHz

Systematic residuals only: $E_{for,syst} = 0.03$

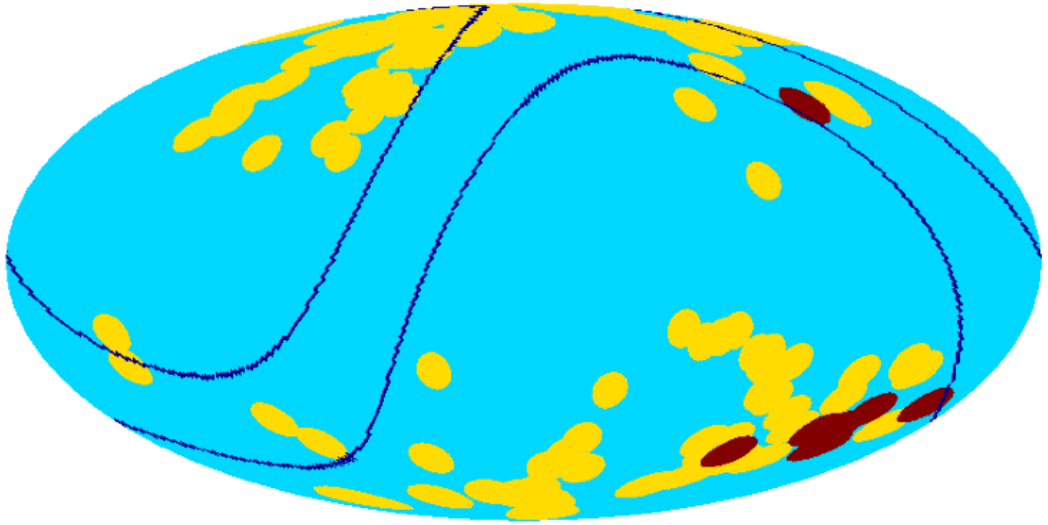

Blue lines corresponding to Dec of 30◦, 0◦
(Galactic coords, Mollweide projection)

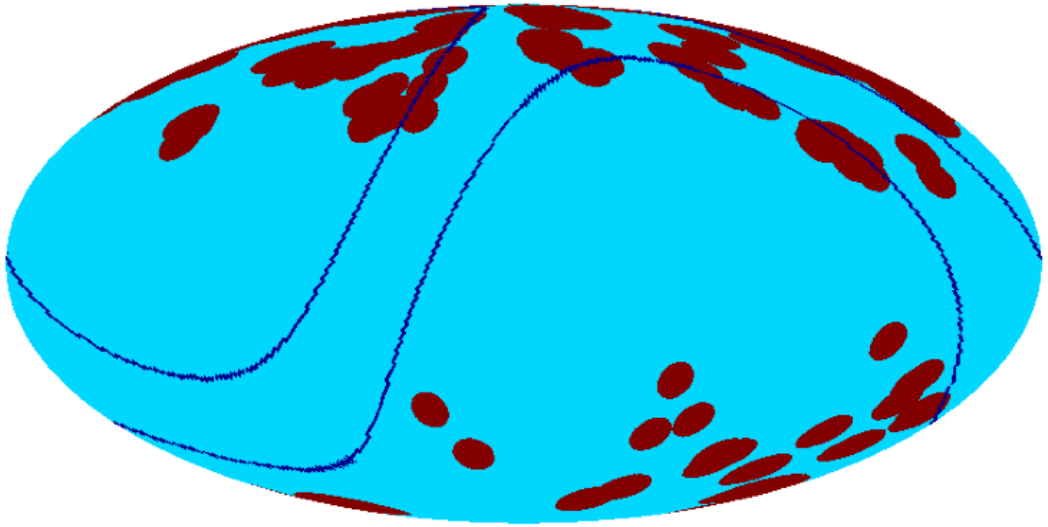

100 MHz - Rel Err on v <= 20%
78 and 61 patches
respectively for the two cuts in declinations,
with a retrieved relative error on β, on average,
of about 15%

1.355 GHz - Rel Err on v <= 85%
60 and 40 patches
respectively for the two cuts in declinations,
with a retrieved relative error on β, on average,
of about 84%

"Good" sky regions - Results @ 100 MHz & 1.355 GHz

Combination of stochastic & systematic residuals: $E_{for} = 0.03$ & $E_{for,syst} = 0.01$

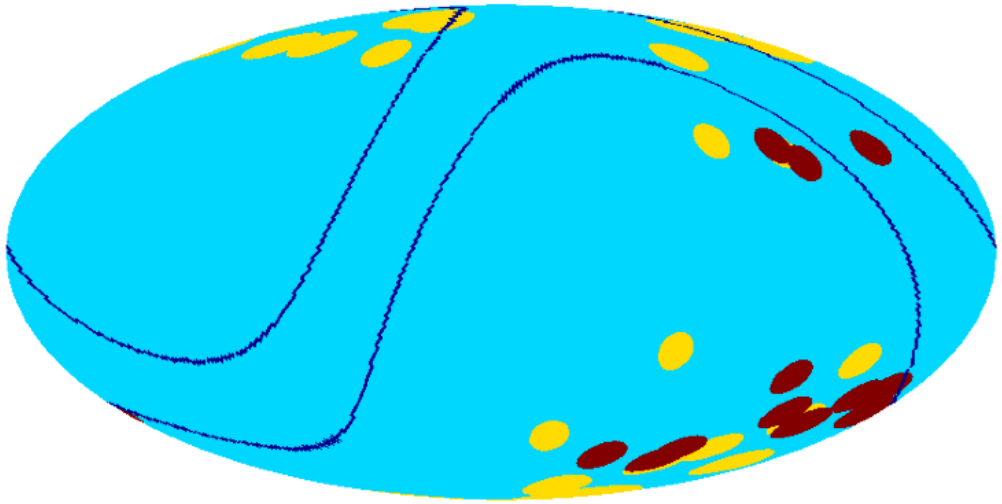

Blue lines corresponding to Dec of 30◦, 0◦
(Galactic coords, Mollweide projection)

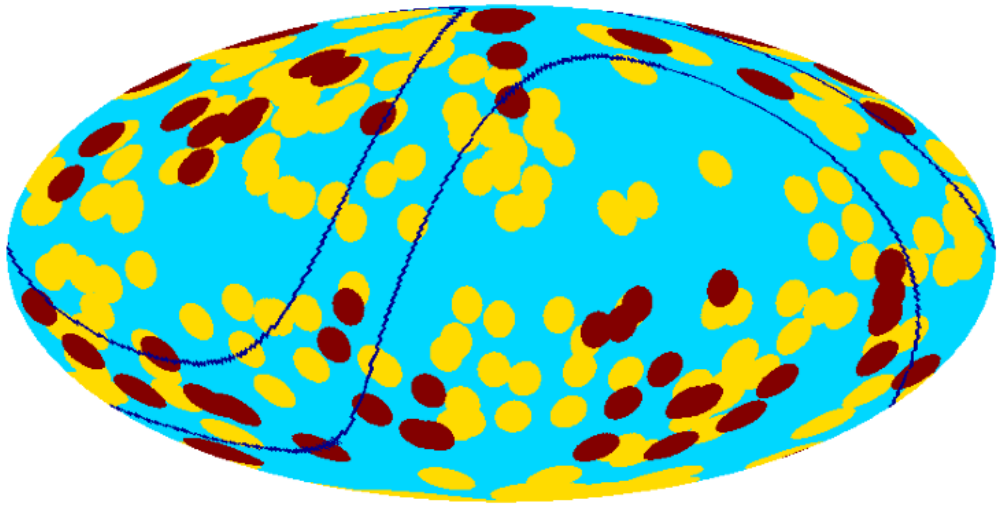

100 MHz - Rel Err on v <= 5%

25 and 23 patches

respectively for the two cuts in declinations, with a retrieved relative error on β, on average,

of about 4.2%

Red: most favourite patches, relative error less than 1.2 x minimum relative error (≃3.5%)

1.355 GHz - Rel Err on v <= 50%

146 and 96 patches

respectively for the two cuts in declinations, with a retrieved relative error on β, on average,

of about 37%

Red: most favourite patches, relative error less than 1.2 x minimum relative error (≃26%)

Conclusions

- **Differential methods relying on precise interfrequency calibration are promising**
- **For observations at extreme sensitivity/resolution, the differential method can be applied to sky patches or limited sky areas, as e.g. in the case SKA interferometric observation, for analyses on background spectra and tests on cosmic dipole**

- **The integrated signal from Extragalactic Sources (likely) gives the major contribution to the CRB**

  dipole analyses compared with estimates for various high flux density limits will test consistency of dipole/monopole versus β from CMB

- **Extracting dipole/monopole information from diffuse CRB on selected sky patches / areas:**
  - **testing v at few or some % accuracy level is feasible …**
  - **provided that residuals of Galactic diffuse emission are within or below a few %**

- **Collecting many patches (or observing a large sky area) allows:**
  - **at least: improvement of S/N**
  - **furthermore: exploiting larger angular scales directly improves sensitivity on dipole**

- **Frequency modulations of CRB dipole spectrum are informative β for other types of signals, tomographic in nature (21cm) or mainly contributed at certain redshifts**